William B. Roberts
Airfoil Technologies International
and Flow Application Research,
Freemont, CA 94539
e-mail: bbclipper@hotmail.com

Scott A. Thorp
National Aeronautics and Space Administration,
Glenn Research Center,
Cleveland, OH 44135
e-mail: Scott.A.Thorp@nasa.gov

Patricia S. Prahst
AP Solutions,
Solon, OH 44135
e-mail: Patricia.S.Prahst@nasa.gov

Anthony J. Strazisar
National Aeronautics and Space Administration,
Glenn Research Center,
Cleveland, OH 44135
e-mail: Anthony.J.Strazisar@nasa.gov

The Effect of Ultrapolish on a Transonic Axial Rotor

Back-to-back testing was done using NASA fan rotor 67 in the Glenn Research Center W8 Axial Compressor Test Facility. The rotor was baseline tested with a normal industrial root-mean-square (RMS) surface finish of 0.5 μm to 0.6 μm (20 microinches to 24 microinches) at 60, 80, and 100% of design speed. At design speed the tip relative Mach number was 1.38. The blades were then removed from the facility and ultrapolished to a surface finish of 0.125 μm (5 microinch) or less and retested. At 100% speed near the design point, the ultrapolished blades showed approximately 0.3% to 0.5% increase in adiabatic efficiency. The difference was greater near maximum flow. Due to increased relative measurement error at 60 and 80% speed, the performance difference between the normal and ultrapolished blades was indeterminate at these speeds. [DOI: 10.1115/1.4006496]

Introduction

As fuel costs continue to increase, the industries that use gas turbine engines have a pressing need to improve in-service performance. This need is especially true in the airline industry, for which fuel burn and performance retention in high by-pass ratio turbofan engines is a major concern. Any approach to improve the efficiency of present equipment will be considered if cost effective.

Previous research by Suder et al. [1] has shown that surface finish of axial fan and compressor blading is very important. This earlier research indicates that there is a significant performance penalty if the surface finish degrades from an industry-standard RMS finish of 0.5 μm to 0.6 μm (20 microinches to 24 microinches) to a finish of 2.5 μm to 3.0 μm (100 microinches to 125 microinches). Figure 1, taken from Suder et al. [1], shows the impact of surface roughness of 2.5 μm to 3.0 μm on the design speed performance of a transonic compressor rotor. The six configurations shown in this figure differ in the location of roughness on the blade surface. One key finding from this work was that surface roughness on the leading edge of the blade, which exists for configurations G, H, and I, causes the most severe performance penalty. Suder's work leads to the question of whether or not a gain in efficiency could be achieved if axial fan and compressor blade surfaces are polished to finishes less than 0.5 μm to 0.6 μm.

According to Koch and Smith [2], the blade surface is considered hydraulically smooth for equivalent sand roughness Reynolds number less than 90. In theory, a better (lower RMS) finish than hydraulically smooth offers no benefit to performance. The standard industry surface finish of 0.5 μm to 0.6 μm is typically near or less than a roughness Reynolds number of 90 at high altitude cruise operating conditions where most fuel burn occurs. At the test conditions used in this work, a surface finish of 0.125 μm (5.0 microinches) corresponds to a roughness Reynolds number of approximately 20. Therefore, there is some justified skepticism as to whether ultrapolish, defined as a surface finish of 0.125 μm or better, can improve efficiency. However, occasional airline trials

with ultrapolished blading have indicated that ultrapolishing is beneficial in that lower fuel burn is observed during acceptance testing after engine refurbishment. To verify and quantify the impact of ultrapolished surface finish on blade performance, back-to-back testing was done in the NASA Glenn Research Center's W8 Axial Compressor Test Facility using NASA fan rotor 67. Baseline testing at a nominal surface finish of 0.5 μm (20 microinches) was followed by testing with the blades ultrapolished to 0.125 μm (5 microinches) or better at 60, 80, and 100% of design speed.

Test Rotor

NASA rotor 67 is shown in Fig. 2. It is a low-aspect-ratio design and the first-stage rotor of a two-stage fan. A complete description of the aerodynamic design of the full two-stage fan is given in Refs. [3] and [4].

The rotor design pressure ratio is 1.63 at a mass flow of 33.35 kg/sec. The design rotational speed is 16,043 rpm, which yields a tip speed of 429 m/sec and an inlet tip relative Mach number of 1.38. The rotor has 22 blades and an aspect ratio of
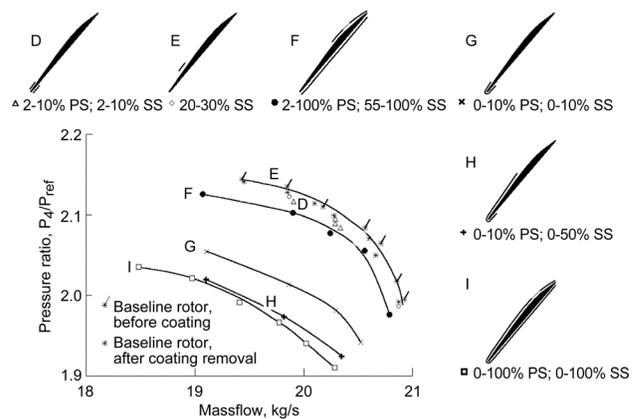
Fig. 1 Pressure rise characteristics of a transonic compressor rotor as a function of the extent of surface roughness, from Suder [1]
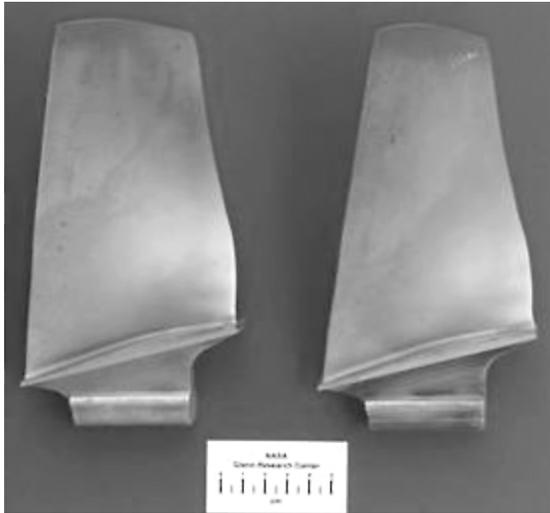
Fig. 2 NASA fan rotor 67
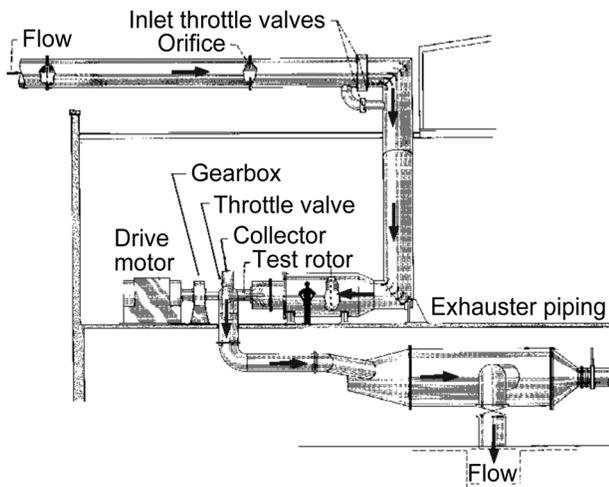
Fig. 3 Schematic diagram of the NASA Glenn Axial Compressor Test Facility

1.56 (based on average span/root axial chord). The rotor solidity varies from 2.11 at the hub to 1.29 at the tip. The inlet and exit tip diameters are 51.14 and 48.5 cm, respectively, and the inlet and exit hub/tip radius ratios are 0.375 and 0.478, respectively. A fillet radius of 1.78 mm is used at the airfoil–hub juncture. The square root of the mean square of the airfoil surface finish is 0.6 μm (24 microinches) or better, the airfoil surface tolerance is ± 0.04 mm, and the running tip clearance is approximately 0.5 mm.

Test Facility

A schematic diagram of the NASA Glenn Axial Flow Compressor Test Facility is shown in Fig. 3. The drive system consists of a 7000 hp electric motor with a variable-frequency power supply. Motor speed is controllable from 400 rpm to 3600 rpm. The motor is coupled to a 5.25 gear ratio speed increaser gear box that in turn drives the rotor. The facility is sized for a maximum airflow of 45 kg/sec with atmospheric air as the working fluid.

Air is drawn into the facility from an inlet located on the roof of the building. The air first passes through a 10 μm filter to remove large particles. An alternate dry-air source can also be used to supply air to the facility. This source was used in the present work to eliminate humidity variations between testing of the
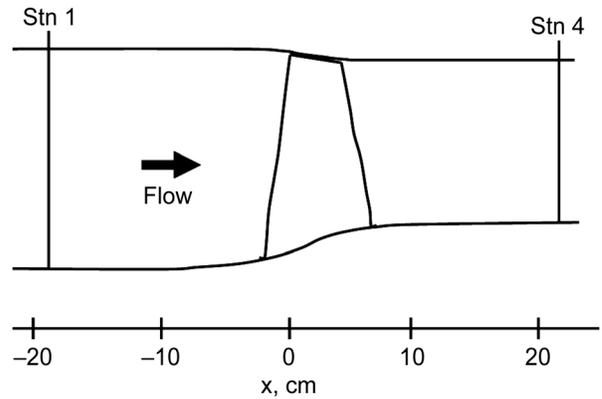
Fig. 4 Location of aerodynamic survey measurement stations

baseline and ultrapolished blading. The inlet air passes through a flow measuring station consisting of a thin-plate orifice, through inlet throttling valves, and into a settling chamber. The air is accelerated into the compressor test section through a nozzle, passes through the test rotor, and then passes through a sleeve valve into a collector before it is exhausted back into the atmosphere. The airflow is controlled through the sleeve valve.

Instrumentation and Measurement Techniques

Mass flow is measured using a calibrated orifice located far upstream of the compressor. The orifice measurements are corrected to standard-day conditions based on settling chamber temperature and pressure. Radial distributions of total and static pressure and flow angle are measured using rakes at stations 1 and 4 shown in Fig. 4. Stage 67 was operated in a rotor-only mode without the stator installed in the present work. Station 4, which is normally used to survey the stator outlet flow, is, therefore, the first available aerodynamic survey station downstream of the rotor. The rake measurements are corrected for streamline slope based on a calibration of each probe used and on the design streamline slope. All rake measurements are corrected to sea-level standard-day conditions in the settling chamber. Radial distributions of total pressure are energy averaged by converting them to their enthalpy equivalents and then mass averaging them across the annulus. Rotor efficiency is determined using the pressure and temperature rise measured across the rotor by the station 4 rakes. Measurement uncertainties are: mass flow, ± 0.11 kg/s; flow angle, ± 0.5 deg; total pressure, ± 0.01 N/cm^2; torque ± 11.5 cm-kg (10 in.-lb).

Test Results

The compressor characteristics for rotor 67 with the baseline and ultrapolish surface finish are shown for 60, 80, and 100% of design speed in Fig. 5. Performance of the baseline configuration was not measured at flow rates near stall because of a concern on maintaining rotor balance during a stall. The performance was measured all the way to stall for the ultrapolished configurations at 80 and 100% speed.

The error bars in Fig. 5 indicate estimated uncertainties in the calculated quantities based on a propagation of error analysis using the measurement uncertainties. The measurement uncertainties at 60 and 80% speed are large due to the decreased relative instrument sensitivity that results from the lower pressure and temperature rise at these speeds. The differences in performance curves for 60 and 80% speed are small between the baseline and polished blades.

At 100% speed performance differences between the baseline and ultrapolished rotor are discernible and are larger than the measurement uncertainties. At design speed the results would seem to imply that the maximum flow capacity of the ultrapolished rotor

Fig. 5 Pressure rise characteristics for baseline and ultrapolished surface finishes
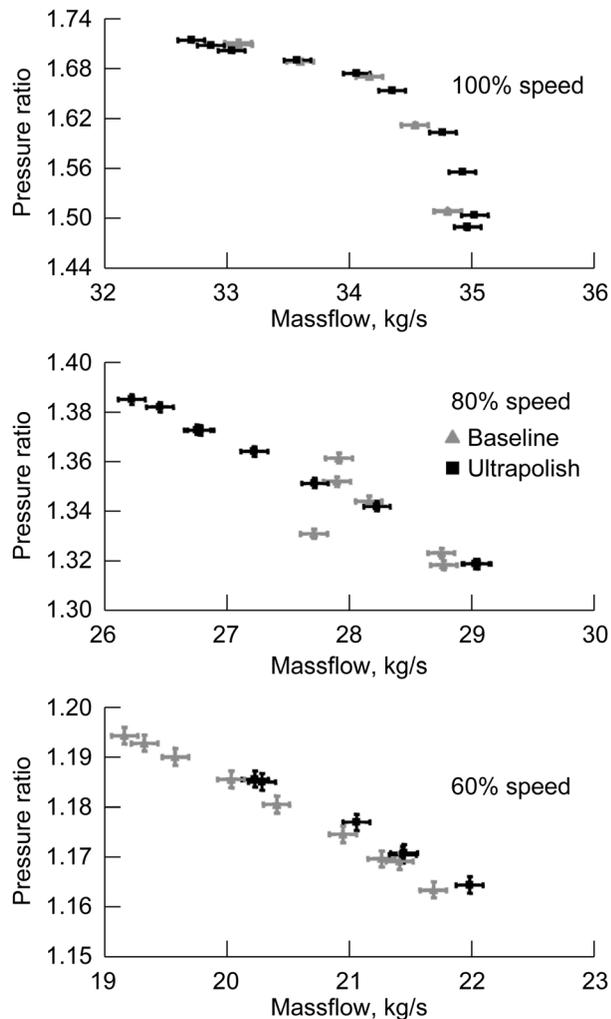
Fig. 6 Adiabatic efficiency characteristics for baseline and ultrapolished surface finishes

is higher than that of the baseline rotor. We are not certain if this is true since the rotor was not yet choked at the lowest backpressure measured for either surface finish. We do note, however, that the trend toward higher flow capacity as the surface finish improves is consistent with the trend observed by Suder et al. [1], as shown in Fig. 1.

We also note that the pressure ratio at the design operating condition is significantly higher than the design value of 1.63. This rotor was designed in the mid 1970s, before the availability of accurate turbomachinery performance prediction capability. The pressure ratio measured in the present work is consistent with that measured and predicted using 3D Navier–Stokes simulations for this rotor by Pierzga and Wood [5].

The main purpose of this research is to determine the difference in adiabatic efficiency between the baseline and ultrapolished blades. Figure 6 shows the adiabatic efficiency plotted versus corrected mass flow for baseline and ultrapolished blades at 60, 80, and 100% speed with error bars calculated using the same propagation of error method as used for the data in Fig. 5.

Discussion

The results in Fig. 6 indicate a noticeable difference between baseline and ultrapolish efficiency, with the ultrapolish blades showing a small but significant increase. For 100% speed, the difference near the maximum efficiency condition is approximately 0.5%. For the lower speeds the efficiency difference is greater: At

80% speed the difference is approximately 1% higher for the ultrapolish case and at 60% speed it is higher by approximately 1.5%. The increasing difference between the baseline and ultrapolish efficiency shown for the various speeds in Fig. 6 is due mostly to the difference in shock system strength with speed. At 100% speed the tip Mach number is approximately 1.38, the relative supersonic inlet flow covers more than one-half of the span, and shock losses dominate. At 80% speed the tip Mach number is approximately 1.1 and relative supersonic flow is confined to the tip region. For 60% speed there is no supersonic inlet flow ($M_{tip} = 0.83$). For the latter two speeds the profile loss is a greater proportion of the overall loss than for design speed. The smoother surface of the ultrapolish blade, therefore, contributes more efficiency increase at the lower speeds.

The speed range for the performance testing is an approximate representation of the cold section of a turbofan engine: 100% speed duplicates the flow regime experienced by the fan; 80% speed the front of a modern high pressure compressor (HPC); 60% speed the rear of an HPC. Consequently the effectiveness of ultrapolish improves from the fan through the HPC outlet.

Although the results in Fig. 6 indicate that the difference in efficiency is greater at higher mass flow conditions, especially at 100% speed, transonic fans in service operate near maximum efficiency. Therefore, the improvement in performance seen by an engine in service would likely be on the order of 0.5% rather than the larger values shown for higher mass flow. The larger
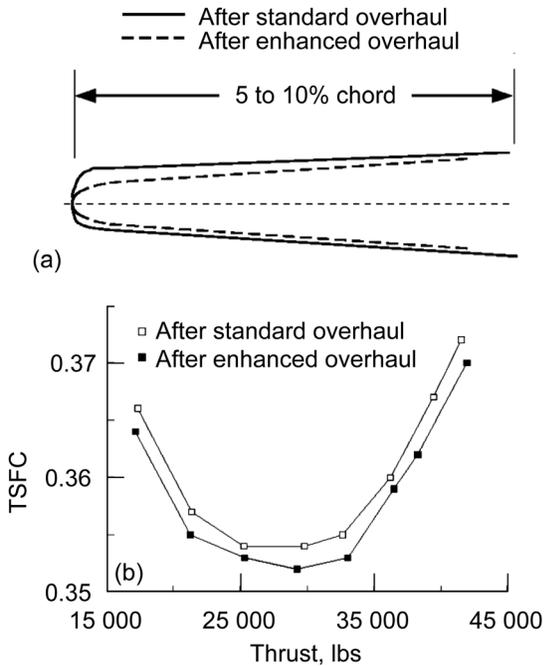
Fig. 7 Impact of leading edge shape on the thrust-specific fuel consumption of a high by-pass ratio turbofan engine, from Roberts [6]. (*a*) Blade leading edge shape before and after enhanced refurbishment. (*b*) Comparison of thrust-specific fuel consumption before and after enhanced refurbishment.

Fig. 8 Magnified photograph of rotor 67 leading edge before and after ultrapolishing

Fig. 9 Measured blade leading edge profile before and after ultrapolishing

efficiency differences observed at high mass flow rates are likely due to changes in the oblique rotor shock strength around the baseline and ultrapolished leading edge.

References [1] and [6] indicate that the leading edge of axial blading can have a significant impact on aerodynamic performance, with rough, oversized, or blunt leading edges significantly decreasing performance. Figure 7, taken from Roberts [6], shows the impact of fan blade leading edge shape on thrust-specific fuel consumption of a high bypass ratio turbofan engine.

Figure 8 shows a photographic magnification of the leading edge of rotor 67 before and after ultrapolish. Although the leading edge of the ultrapolished blade is not perfectly smooth, the surface finish is more uniform than the baseline leading edge. The ultrapolish process does remove a very small amount of material from the surface of the blade. Therefore, if the ultrapolish process improved the leading edge of the blades by smoothing or decreasing the thickness, all or part of the efficiency increase shown in Fig. 6 could be from leading edge shape change.

To check the sensitivity of rotor 67 performance to leading edge shape, a quasi three-dimensional computational analysis was performed on the blade geometry at 100% design speed. The 70% span location (from the hub) was chosen for this analysis since it is well outside the endwall region but well within the transonic region, i.e., relative inlet Mach number at design speed equal to 1.15. A composite blade shape for the baseline and ultrapolish blades was derived by averaging the measurements acquired from the 22 individual blades by a coordinate measuring machine at 70% span for pre- and postpolished cases. These composite blade profiles are shown in Fig. 9, where no significant difference in leading edge shape can be seen. The coordinate measuring machine accuracy is on the order of 0.005 mm, which is smaller than the data point symbol size in Fig. 9. Note that the ultrapolished blade is actually thicker than the baseline blade near the leading edge because the ultrapolish process removed a small amount of material from the nose of the blade; thus effectively blunting the nose of the airfoil.

From Fig. 5, it can be seen that there are two data points at design speed for the baseline and ultrapolished cases that have
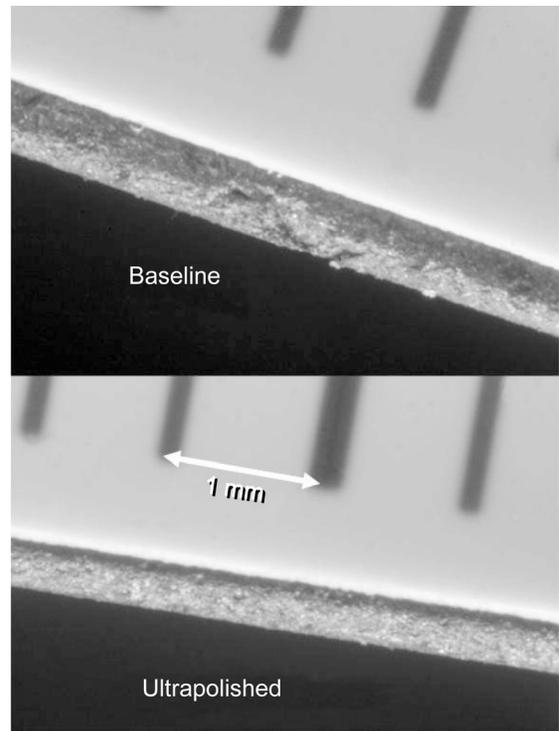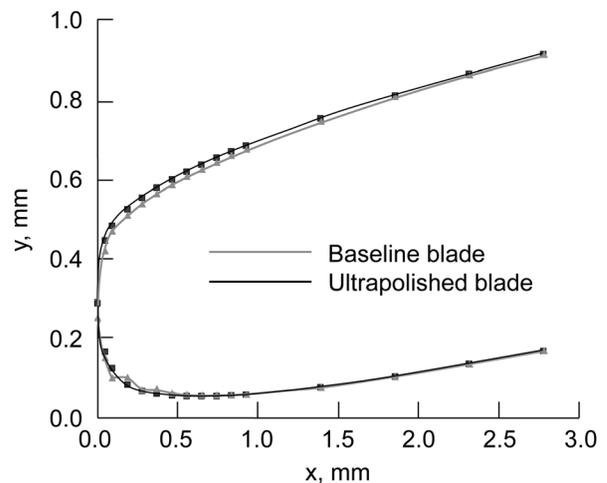
nearly the same corrected mass flow of 33.56 kg/sec (74 lb./sec). This means that inlet-air angles and inlet-relative Mach numbers are the same for both cases. However, there is a measured difference of 0.65% in efficiency between these points (see Fig. 6) due either to surface finish or leading edge shape.

A numerical analysis of the flow over the pre- and postpolish composite profiles was performed for this mass flow rate using the quasi three-dimensional Navier–Stokes solver developed by Chima [7]. This code has previously been used to predict streamtube loss coefficient for the transonic fan of a large production high-bypass turbofan engine. The computation using the code predicted measurement within $\Delta\bar{\omega} = 0.0003$ [8].

The relative inlet-air angle and Mach number at 70% span was deduced from the measured inlet total and static pressure, plenum temperature, and rotational speed. The outlet static to inlet total
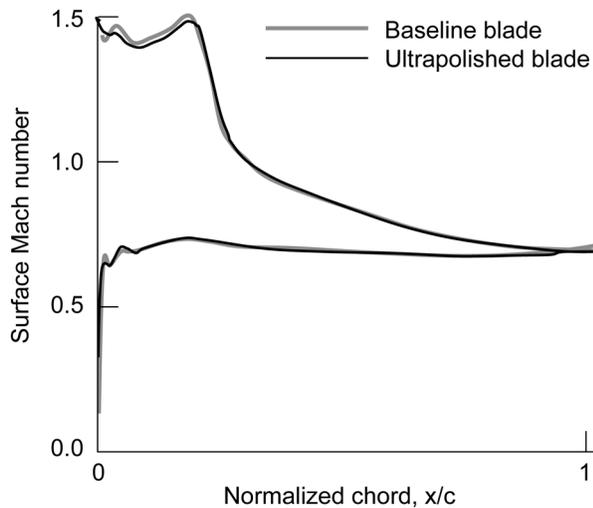
Fig. 10 Comparison of predicted surface Mach number distribution at 70% span from the hub at design speed using blade geometry as measured before (baseline) and after ultrapolish

Table 1 Summary of rotor 67 blade element performance predictions for the baseline and ultrapolished geometry at 70% of span from the hub at 100% speed

Parameter	Baseline	Ultrapolish
M_1	1.15	1.15
β_1 (deg)	65.6	65.6
β_2 (deg)	57.9	57.7
θ (deg)	7.6	7.9
$\bar{\omega}$	0.11798	0.11624
Δm (%)	0.1784	0.03264

pressure ratio was adjusted to minimize the mass flow residual $\Delta\dot{m}$. The results are shown in Fig. 10 and Table 1.

It can be seen that the inlet and outlet Mach numbers, flow angles, total pressure loss coefficients, and surface Mach number distributions are essentially the same. The two main performance parameters, total pressure loss coefficient, $\bar{\omega}$ and flow turning θ are slightly different. The difference between computed loss coefficients is $\Delta\bar{\omega} = 0.11798 - 0.11624 = 0.00174$.

From aerothermodynamic analysis and industrial experience it is known that a 1% change in blade element loss coefficient over a high pressure compressor leads to approximately 1% change in adiabatic efficiency. Therefore, the efficiency increase predicted by the quasi three-dimensional analysis due to airfoil leading edge changes after ultrapolishing is 0.00174 or 0.174%. This is about one-fourth of the measured improvement in efficiency. The predicted difference in flow deflection before and after ultrapolishing is 0.3 deg, which is well within the manufacturing tolerance of ± 1 deg for rotor 67 blading. Therefore, we conclude that the efficiency improvement after ultrapolishing shown in Fig. 6 at design speed is due to the surface finish change.

Figure 11 presents spanwise distributions of adiabatic efficiency measured with the downstream rakes. The data is the average of data collected over three separate runs. For all cases the corrected mass flow was 33.56 ± 0.06 kg/sec with speed held at 100%. Inflow Mach numbers and flow angles are therefore the same for all data. Comparison of the two dry-air cases in Fig. 11 shows a mass-averaged efficiency difference of approximately 1% in favor of the ultrapolish case.

As blades foul in service, the efficiency of the compression system eventually drops off. The ability of a rotor to retain the ultrapolish efficiency gain in service is, therefore, a valid concern. We assessed this issue by checking the performance of this rotor after
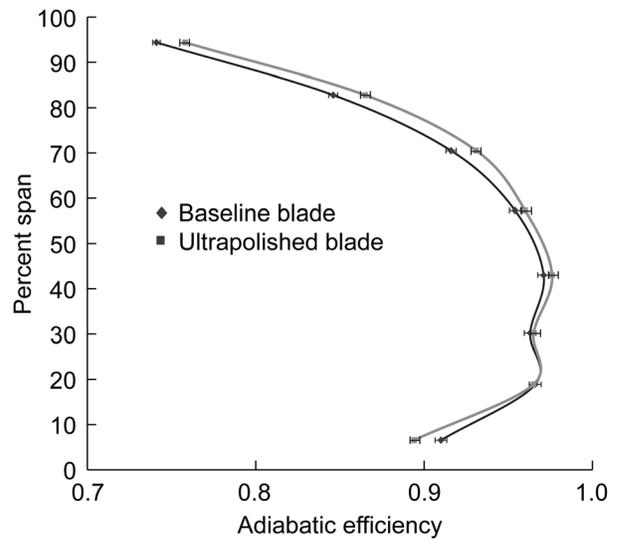
Fig. 11 Spanwise profile of adiabatic efficiency for baseline and ultrapolished blade in dry air at 100% speed
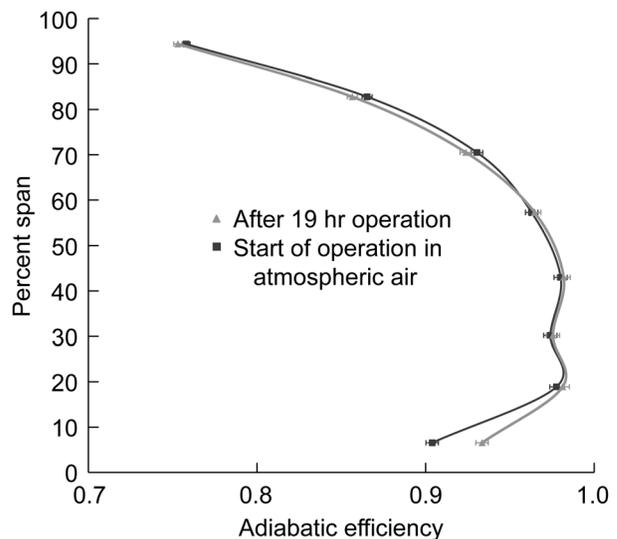
Fig. 12 Spanwise profile of adiabatic efficiency for ultrapolished blade at start of operation in atmospheric air and after 19 h of operation in atmospheric air at 100% speed

the completion of a test program that followed the present work. The rotor was operated for 13 months in the follow-on program during which it accumulated 19 h (1140 min) of operation at design speed. Throughout this follow-on program, the rotor was supplied with atmospheric air, filtered to 10 μm. Figure 12 is a comparison of the spanwise distribution of efficiency at the start of operation in atmospheric air to that measured after 19 h of operation in atmospheric air, showing no measureable change in performance. For both cases the corrected mass flow was once again 33.56 ± 0.06 kg/sec with speed held at 100%.

A commercial aircraft engine operates at full-speed only during the takeoff climb and during thrust reversal at landing. Furthermore, there are substantially fewer atmospheric particles that can foul blades above 10,000 ft. A commercial engine therefore spends only 4 min to 5 min per flight at design speed at altitudes where atmospheric particulates are a concern. The 19 h (1140 min) of operation accumulated by the rotor before the performance was rechecked therefore represent 250 cycles to 300 cycles.

Table 2 Spanwise distribution of adiabatic efficiency. Comparison between baseline and ultrapolished rotor in dry air and between ultrapolished rotor before and after 19 h of run time in atmospheric air at 100% speed

% span	Baseline dry air	Ultrapolish dry air	Ultrapolish at start of atmos. air	Ultrapolish after 19 h atmos. air
94	0.741	0.758	0.758	0.753
83	0.846	0.865	0.866	0.857
71	0.916	0.931	0.930	0.924
57	0.954	0.960	0.963	0.965
43	0.971	0.976	0.980	0.982
30	0.963	0.965	0.974	0.976
19	0.966	0.965	0.978	0.981
7	0.910	0.894	0.904	0.934
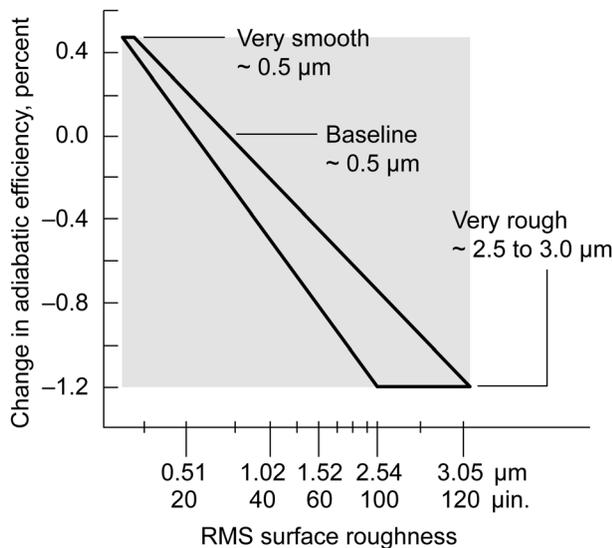
Fig. 13 Approximate variation of adiabatic efficiency with surface finish for transonic rotors

The results plotted in Figs. 11 and 12 are tabulated in Table 2. All columns in Table 2 are the average of three runs except the last, which is from one run.

Suder et al. [1] measured the efficiency change of a transonic core compressor rotor when surface roughness was increased *above* the industry-standard surface finish level of 0.5 μm to 0.6 μm. In the present work we have investigated the efficiency change of a transonic fan rotor when the surface roughness level was decreased *below* industry-standard levels. We have found that these results are in line with one another as shown in Fig. 13, which combines the efficiency changes measured by Suder with those measured in the present work. This semilogarithmic plot shows the trend in adiabatic efficiency change with surface finish for transonic rotors.

Conclusions

NASA rotor 67 has been tested with an industry-standard surface finish of 0.5 μm (20 microinches), ultrapolished to a 0.125 μm (5 microinches) finish, and retested. An approximate increase in efficiency of 0.5% was measured for the ultrapolished rotor near maximum efficiency at design speed.

An increase in efficiency on the order of 0.5% across the fan and compressor reduces the exhaust gas temperatures by 5 °C to 8 °C, resulting in increased time in service. A typical medium-size turbofan engine such as the PW2037 or the CFM56 burns between 1.5 and 2 × 10^6 gallons of fuel per year in regular airline service

[9]. At present day fuel prices it would take approximately 1 month to pay back the cost of ultrapolishing if the process yields a 0.5% reduction in fuel burned. After the payback period, the fuel cost savings would be $22,000 to 30,000 per engine per year (at a fuel cost of $3.00/gal.).

Acknowledgment

Nomenclature

s/c = space/chord ratio
M_1 = inlet relative Mach number
X = distance along the chord line
Y = distance normal to the chord line
PR = total pressure ratio
PS = pressure surface
SS = suction surface
TSFC = thrust-specific fuel consumption
$\Delta\dot{m}$ = mass flow residual, quasi three-dimensional calculation
β_1 = inlet relative air angle
β_2 = exit relative air angle
θ = airflow turning through the blading
$\bar{\omega}$ = total pressure loss coefficient

References

[1] Suder, K. L., Chima, R. V., Strazisar, A. J., and Roberts, W. B., 1995, "The Effect of Adding Roughness and Thickness to a Transonic Axial Compressor Rotor," ASME J. Turbomach., **117**, pp. 491–505.
[2] Koch, C. C., and Smith, L. H., 1976, "Loss Sources and Magnitudes in Axial Flow Compressors," ASME J. Eng. Power, **98**(3), pp. 411–424.
[3] Cunnan, W. S., Stevens, W., and Urasek, D. C., 1978, "Design and Performance of a 427 Meter-per-Second-Tip Speed Two-Stage Fan Having a 2.40 Pressure Ratio," NASA TP-1314.
[4] Urasek, D. C., Gorrell, E. T., and Cunnan, W. S., 1979, "Performance of Two-Stage Fan Having Low-Aspect-Ratio, First-Stage Rotor Blading," NASA TP-1493.
[5] Pierzga, M. J., and Wood, J. R., 1985, "Investigation of the Three Dimensional Flow Field Within a Transonic Fan Rotor: Experiment and Analysis," ASME J. Eng. Gas Turbines Power, **107**(2), pp. 436–449.
[6] Roberts, W. B., 1995, "Advanced Turbofan Blade Refurbishment Technique," Technical Brief, ASME J. Turbomach., **117**, pp. 666–667.
[7] Chima, R. V., 1987, "Explicit Multigrid Algorithm for Quasi-Three-Dimensional Viscous Flows in Turbomachinery," AIAA J. Propul. Power, **3**(5), pp. 397–405.
[8] Roberts, W. B., 1994, "The Effect of Recontouring GE CF6-80C2 Fan Blades," FAR Technical Note prepared for Sermatech International and KLM Royal Dutch Airlines.
[9] Justice, J., 2004, Private communication.